

# Vanishing exchange and the emergence of a pseudo-spin in restricted momentum space multi-electron atoms

G.P. Lansbergen<sup>1,\*</sup>, R. Rahman<sup>2,3</sup>, J. Verduijn<sup>1</sup>, G.C. Tettamanzi<sup>1</sup>,

N. Collaert<sup>4</sup>, S. Biesemans<sup>4</sup>, G. Klimeck<sup>2,5</sup>, L.C.L. Hollenberg<sup>6</sup>, and S. Rogge<sup>1</sup>

<sup>1</sup>*Kavli Institute of Nanoscience, Delft University of Technology, Lorentzweg 1, 2628 CJ Delft, The Netherlands*

<sup>2</sup>*Network for Computational Nanotechnology, Purdue University, West Lafayette, Indiana 47907, USA*

<sup>3</sup>*Sandia National Laboratories, Albuquerque, NM 87185, USA*

<sup>4</sup>*InterUniversity Microelectronics Center (IMEC), Kapeldreef 75, 3001 Leuven, Belgium*

<sup>5</sup>*Jet Propulsion Laboratory, California Institute of Technology, Pasadena, California 91109, USA and*

<sup>6</sup>*Center for Quantum Computer Technology, School of Physics, University of Melbourne, VIC 3010, Australia*

(Dated: May 24, 2022)

The observation and characterization of single atom systems in silicon [1–7] is a significant landmark in over a half century of device miniaturization, and presents a new laboratory for fundamental atomic physics. Impurity atoms locked in a silicon matrix offer a unique opportunity to study the effects of momentum space restrictions on the construction of multi-electron atomic states, and external control of essential atomic quantities and phenomenon not accessible to the well-known vacuum forms. We report the first measurement of the spectrum of a single isolated defect atom in silicon filled with two electrons, uncovering bound states not previously observed and the emergence of pseudo-spin as a new quantum number. This work is an important step forward in establishing the fundamentals of tunable multi-electron atom physics in the solid-state as a laboratory for a range of atomic phenomena under novel conditions, as well as a promising source of new device technology.

We normally think of fundamental atomic properties such as the nuclear Coulomb potential, uniform momentum space and transition selection rules as fixed at a very deep level by the laws of nature. Certainly, for isolated atoms in vacuum this is indeed the case. However, the rapid confluence of quantum technology and device miniaturization has presented new opportunities to study atomic physics in situations where not only the rules of vacuum atomic physics no longer apply, but the rules themselves can be engineered. The ability to fabricate, control and characterize single atomic defect systems in the solid-state [8–16] present such opportunities for the design and study of fundamental atomic physics in ways not accessible previously to the vacuum counterparts. Single impurities represent more than the ultimate limit of spatial electronic confinement in the solid state compared to heterostructure or electrostatic gate confined quantum dot systems - the impurity system is confined by a Coulomb potential and hence fundamentally related to the vacuum atom case. Thus, these atoms in a solid-state matrix offer a unique laboratory to study the quantum mechanics of atoms under extraordinary conditions.

Atomic systems in silicon present a particularly alien phenomenology compared to the vacuum counterpart, see Fig.1. In vacuum the localization of the electron in the confining potential is able to access all values of momentum in the usual wave-packet derived from the 1s Bohr orbital. However, when the atom is embedded in a silicon host the electron's momentum is constrained by the symmetry of the crystalline host, and one must take into account the very different dispersion relation corresponding to the six degenerate minima (valleys) at non-

zero momentum values along each cartesian direction. Not only is the confining potential susceptible to tuning by external controls or boundary conditions, but the basic atomic properties like Hund's rule are very different to the vacuum case. For decades these systems could only be studied in the bulk and only in the coarsest terms for samples containing a large number of impurities. It is only recently that a single impurity could be detected and studied for the single electron-atom case [1, 3]. However, the non-trivial atomic physics that comes from the case of two or more electrons has till now been inaccessible and completely unknown, except in the bulk/ensemble sense. In bulk, only one bound state has been observed for the  $D^-$  system [17].

In this paper we study the formation of two-electron states in such an atomic donor in silicon, measuring their bound state spectrum and selection rules. We observe, that in the solid the valleys play the role of a pseudo spin in addition to the common selection rules.

In going beyond the single electron case, this work heralds new opportunities to study atomic device physics as two electrons on a donor form a key element for quantum information processing (QIP) due to the spin selective orbital states which allow for spin to charge conversion [19]. Understanding exchange interaction in a multi-valley semiconductor is a first step to validate the Kane architecture of using exchange to couple adjacent donors. Previous QIP architectures utilized divalent donor [20] or two donors [21] to implement spin to charge conversion because bound triplet states in a single donor were not expected. We demonstrate the latter for a donor-interface system which opens up the way to implement spin to charge conversion with a single shallow donor like

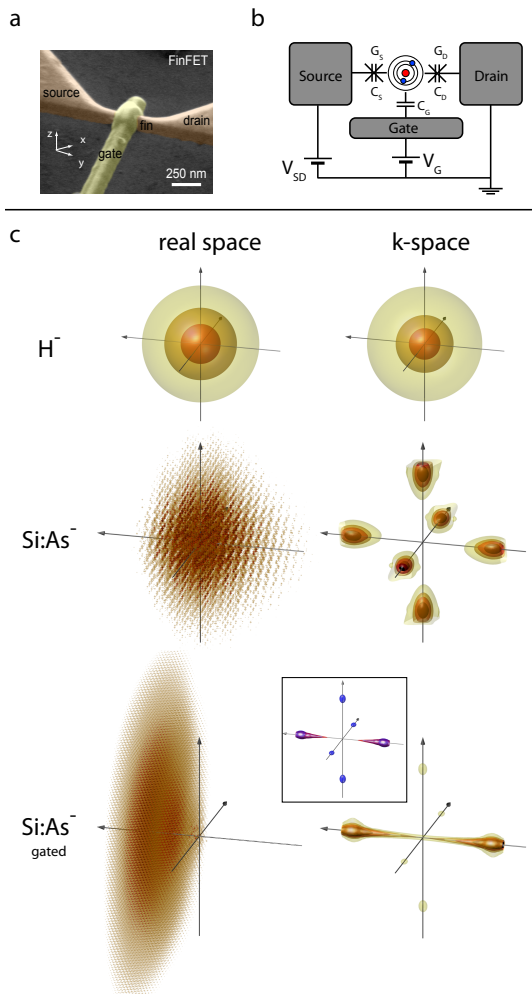


FIG. 1. A single atom system in silicon **(a)** Colored SEM-image of a silicon FinFET device. A nanowire connected to source- and drain -leads (brown) forms the channel of the transistor, where single As donors can be identified in transport measurements. A second silicon nanowire deposited perpendicular to the channel (yellow) forms the gate electrode, which is separate from the channel by a thin nitrided oxide. **(b)** Selected devices effectively act as a single (donor) atom in a three terminal geometry, i.e. coupled to source (S), drain (D) and gate (G) electrodes. The electrically equivalent scheme is in analogy to that of a regular quantum dot. **(c)** Contrasting the differences in wave function density (shown here for the single electron atom only) between lattice bound atoms with non-trivial momentum space structure, and the simpler vacuum counterpart. Multi-million atom tight-binding simulations were employed to calculate the Si:As electron wave functions for comparison. In real space the two are similar besides the oscillation of the Bloch states of the crystal. The difference becomes obvious in  $k$ -space. Due to the indirect band gap of the semiconductor the analog atom resides in the six valleys of the conduction band which has profound effects on the properties of the atom as noted in the spectrum. The presence of a spectrum of  $k$ -states needed to represent the ungated and gated Si:As electron wavefunction in Si is a testimony for the need of a full-band, atomistic representation, rather than an a-priori limitation to a selective set of  $k$ -states such as an effective mass representation.  $k$ -state mixing due to crystal symmetry, electric and magnetic fields is included by choice of a basis set in our modeling.

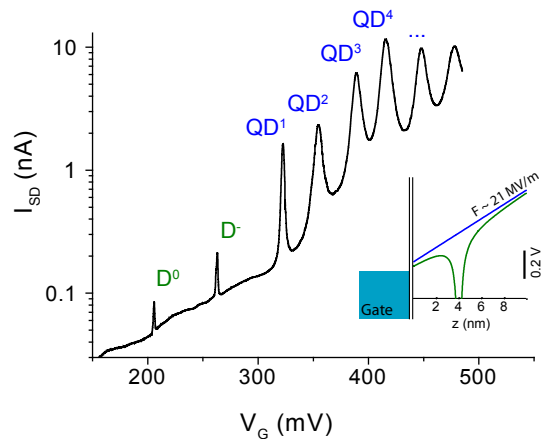


FIG. 2. Coulomb blocked transport in a FinFET transistor. Two separate charge islands can exist inside the transistor; a quantum dot confined by the triangular potential at the gate interface and residual barriers in the access regions between source/drain and channel and a donor/well system confined by the donors Coulomb potential and a well at the interface. The localized states formed in these charge islands are denoted by  $QD^n$  and  $D^0/D^-$  respectively. Inset: The potential landscape in a cross-section from the gate to the channel. The gate electric field induces a triangular potential at the interface (blue). An (accidental) donor atom in the channel forms a Coulombic potential on top of the gate potential (green).

P or As.

Here, we measure the charging energy and the orbital energies of four states of the system. This allows us to study the atomic physics associated with gated donors in a multivalley environment, of which the charging- and orbital -energies are a mere reflection. We obtain detailed understanding of the charging- and orbital -energies within a multi-million atom tight-binding framework, where the electron-electron interaction is taken into account by a self-consistent field Hartree-Fock method. In going beyond effective mass approximations, our method fully captures the prominent valley-orbit interactions without a-priori fitting parameters as valley-orbit interaction is built into the basis states of the problem. The data suggests that the external gate potential has the ability to put the system into a 2D confinement regime in which the electron occupies different valleys of the silicon host lattice for which the exchange coupling is very small. Furthermore, we can experimentally identify an excited state with an exceptionally long life-time ( $> 48$  ns) in the  $D^-$  spectrum by means of a life-time-enhanced-transport mechanism [18]. The long life-time is attributed to the combination of spin- and valley- blockade in the relaxation process, in line with the gate-induced 2D-symmetry we expect it to have from our tight-binding simulations. The valley de-

gree of freedom thus forms a good quantum number in this atomic system.

The valley degree of freedom of the silicon conduction band is also a critical factor in the design of silicon quantum computation schemes [19, 22–24], as only when the valley degeneracy is lifted will the spin lifetime be long enough to allow for coherent operation. Interface confinement by the gate field will lift the degeneracy such that only the two valleys perpendicular need to be considered [25]. The degeneracy of these two valleys is typically lifted by the valley-orbit interaction. In SiGe, the resulting valley-orbit splitting is very dependent on the properties of the interface such as alloy disorder and strain, and is thus hard to control [26–28]. However, for CMOS structures, with their high-quality Si/SiO<sub>2</sub> interfaces, the valley-orbit splitting seems to more predictable [3, 29–31].

The devices used in this study are Si FinFET transistors, consisting of a Si nanowire with a gate covering three faces of the body, see Fig. 1a. We have measured the low-temperature electronic transport of around 100 devices and selected 6 devices where the sub-threshold characteristic are dominated by a single donor atom in the channel, see Fig. 1b. The characteristic fingerprint of a single dopant consist of a pair of resonances associated with the  $D^0$  and  $D^-$  charge states with a binding energy of  $\sim 50$  meV, a charging energy between 30-35 meV and a spin odd-even effect [1]. The other devices either showed no sub-threshold signal or a complicated pattern associated with Coulomb interaction between several donors in the channel. The high electric field transforms the confining potential to a (hybridized) mix between the donors Coulomb potential and a triangular well at the interface, as depicted in the inset of Fig. 2c [3]. This system is thus essentially a gated donor where the donor-bound electrons are partly pulled toward the Si/SiO<sub>2</sub> interface.

Figure 2 shows the source-drain current of device GLG14 (see also Ref. [3]) at low bias as a function of gate voltage. At any gate voltage where a localized state in the channel is within the bias window defined by source/drain, it gives a contribution to the transport and a peak in the current occurs. As such, we can perform spectroscopy, with the gate voltage being a measure for the energy of the level ( $E = \alpha V_G$  where  $\alpha$  is the electrostatic coupling between the gate and the level). Based on the aforementioned criteria, we identify the first two resonances as the  $D^0$  and  $D^-$  charge states of a single As donor. The resonances indicated by  $QD^n$  are due to a localized state which is confined by the gate electric field and two barriers in the access regions between source/drain and the channel [32–34].

Next we analyze the charging energy between the  $D^0$  and  $D^-$  charge states. The charging energy of gated donors can be reduced due to both capacitive coupling to the leads and deformation of the wavefunction density due to the gate field [3]. Figure 3 shows a tight-binding

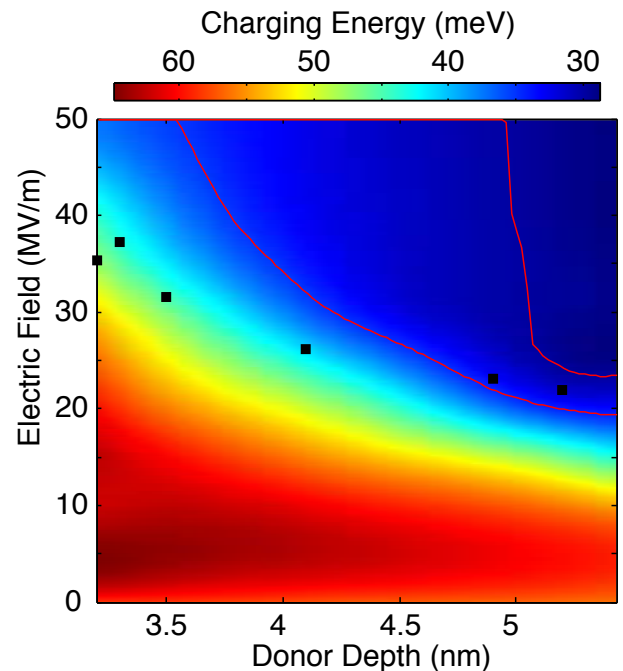


FIG. 3. Colormap of the modeled charging energy as a function of gate electric field ( $F$ ) and donor depth ( $d$ ). The red curves indicate the region where the modeled charging energy is between 30-35 meV, as we also find experimentally. The black data points indicate the positions of 6 samples in the  $F$ - $d$  plane, as determined in a previous publication [3] from their  $D^0$  level spectrum. The discrepancy between modeled and measured charging energy is attributed to capacitive coupling to the gate which will reduce the charging energy, especially for samples close to the interface as observed.

calculation (NEMO-3D [36, 37]) of the charging energy as a function of gate electric field ( $F$ ) and donor depth below the Si/SiO<sub>2</sub> interface ( $d$ ). In going beyond effective mass approximations [35], our full-band, 10 orbital  $sp^3d^5s^*$  tight-binding approach captures valley-orbit interactions in a natural fashion. The Coulomb interaction between the two electrons on the donor site were calculated in a self-consistent field Hartree Fock approach. The calculations include half a million atoms of a significant part of the device, with a volume of 10.2 x 30.4 x 30.4 nm. We chose to set the first dimension of the box at 10.2 nm to take into account the confinement provided by the corner regions of the FinFET, where the donors are located [34]. It should be noted that modeling the corner confinement as if it were a hard-wall box is a rough approximation, which induces a certain degree of uncertainty in final result [27, 28]. At low electric field  $F$  or shallow donor depth  $d$  the sample is donor-like and the charging energy is close to the bulk value of an As donor (52 meV). At high  $F$  or deep  $d$  the donor electron(s) are pulled into the interface well and the charging energy is set by this confining potential ( $\sim 28$  meV, see Fig 3). In between the two latter extremes the charging energy makes a smooth

transition, as can be expected from a hybridized system [45]. It should be noted that the electron(s) in the interface confinement regime are still laterally confined near the donor and should thus not be confused with the  $QD^n$  localized states, which are confined by the barriers in the access regions. The lateral localization of the  $D^-$  state near the donor nucleus can be clearly observed in real-space simulations of the  $D^-$  wavefunction.

In previous work, we determined the  $F$  and  $d$  of six donor samples by means of their  $D^0$  orbital spectrum [3]. The charging energy of these samples was found to be between 30-35 meV, thus lower than the bulk value of 52 meV. These samples are indicated in the  $F$ - $d$  plane of Fig. 3 by the black squares. The red curves in the plot indicate the region where the charging energy is between 30-35 meV theoretically. Thus, we find good agreement between theory and experiment, especially at large donor depth. We attribute the discrepancy at small depth to screening effects of the gate interface. A full self-consistent simulation taking both screening effects *and* valley-orbit interaction and other atomistic details into account is a daunting theoretical and computational challenge that involves the atomistic disordered amorphous  $SiO_2$  interface, on which currently no work exists. Screening by the gate can be considered as capacitive coupling to the environment, increasing the total capacitance of the donor/well site and decreasing the charging energy. This effect should be stronger for donors close to the interface, which correspond to the larger discrepancy we find for these particular samples. There is a good agreement between theory and experiment suggesting a significantly reduced charging energy caused by a combination of the deformation of the donor wavefunction and capacitive coupling to the environment.

Now that we have reviewed the charging energy in our gated donor system, we turn our attention to the orbitals. The orbitals essentially consist of linear combinations of the six valleys of the Si conduction band. In the remaining part of this article we will investigate the  $D^-$  orbital level spectrum and their corresponding spin/valley configurations by analyzing the DC electronic transport. We can observe bound excited states (due to the reduced charging energy) and we can expect that exchange interaction will induce the formation of singlet- or triplet-spin configurations. We already know that the ground state is in a singlet spin configuration, as determined by the magnetic field dependence of the zero-bias resonance [1].

We have determined the temperature dependence of the  $D^-$  transport resonance and analyzed it by a now relatively standard method first described by Foxman *et al.* [38], see Appendix I. As such, we find that the transport is in the sequential limit [39], is very asymmetrically coupled to source and drain, i.e.  $\Gamma_L/\Gamma_R \approx 2000$  and that the  $D^-$  has a low-lying excited state at  $\sim 1$  meV.

To identify excited states at higher energy we inves-

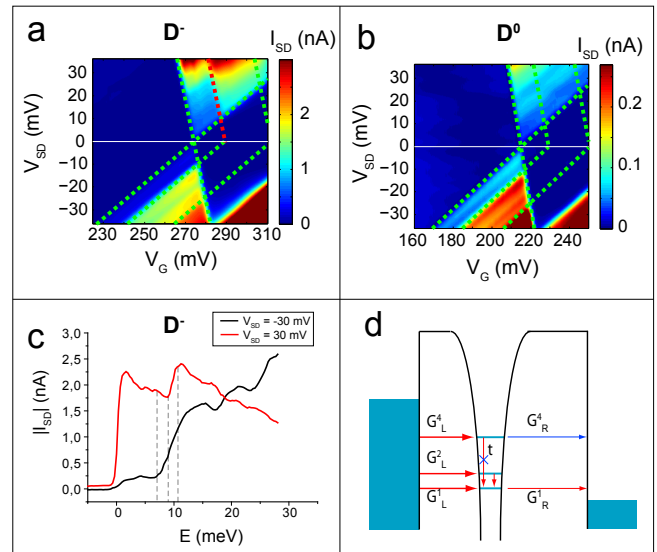


FIG. 4. The excited states of the  $D^-$  can be distinguished by carefully examining the DC transport. **(a)** Stability diagram of the  $D^-$  charge state resonance. The green dashed lines indicate current steps associated with an excited state entering the bias window. The highly asymmetric coupling and the sequential nature of the transport quenches the current steps in the  $V_{SD} > 0$  conducting region (see main text). The current step in the  $V_{SD} > 0$ , associated with the  $n = 3$ -excited orbital, must necessarily have a life-time ( $\tau$ )  $> 48$  ns to show a significant in the DC transport. **(b)** Stability diagram of the  $D^0$  charge state resonance. The green arrows again indicate excited states entering the bias window. No life-time enhanced features are seen in the  $D^0$  charge resonance. **(c)** Source/drain current through the  $D^-$  versus local potential of donor atom  $E$  (with respect to the ground state) for  $V_G = -30$  meV and  $V_G = +30$  meV. **(d)** Transport processes responsible for the current characteristics in our single-atom device. Sequential processes are characterized by relaxation to the ground state before tunneling out of the atom. Due to the long life-time of the  $n = 4$ -state, the electron can tunnel directly out of the state to the drain.

tigate the stability diagram in the current ( $I_{SD}$  versus  $V_G$  and  $V_{SD}$ ) of the sample. Fig. 4a shows the stability diagram around the  $D^-$  charge state. We observe several steps in the conducting region which can be associated with the excited states spectrum [3, 40], indicated by the green dashed lines. These steps are clearly present for  $V_{SD} < 0$  but are absent for  $V_{SD} > 0$ , except for one current step indicated by the red dashed line, supporting the argument of asymmetry being strongly visible in the  $I$ - $V$  characteristics [40]. The current through the donor atom is given by (see also [41])

$$I = e \frac{(\Gamma_{in}^1 + \Gamma_{in}^2 + \dots + \Gamma_{in}^n) \Gamma_{out}^1}{\Gamma_{in}^1 + \Gamma_{in}^2 + \dots + \Gamma_{in}^n + \Gamma_{out}^1} \quad (1)$$

where the subscript denotes the direction of the rate (in or out of the donor), the superscript indicates the level

(where 1 is the ground state) and  $n$  indicates the number of states in the bias window defined by source drain. The total rate into the atom depends on the amount of states in the bias window but the outgoing rate depends only on the rate out of the ground state. This reflects the sequential nature of the tunneling process, as an electron transferred to the atom will have relaxed to the ground state before being transferred to the opposite lead. Allowed relaxation process in silicon donors typically take place within a few  $ps$  [42], much shorter than the tunneling times in our structure. Since the atom in our sample is very asymmetrically coupled,  $\Gamma_{in} \gg \Gamma_{out}$  for  $V_{SD} > 0$  while  $\Gamma_{in} \ll \Gamma_{out}$  for  $V_{SD} < 0$ . In this asymmetric limit Eq. 1 reduces to

$$I = e(\Gamma_{in}^1 + \Gamma_{in}^2 + \dots + \Gamma_{in}^n) V_{SD} < 0 \quad (2)$$

$$e\Gamma_{out}^1 V_{SD} > 0 \quad (3)$$

$$(4)$$

Also for  $D^0$  no steps are observed for  $V_{SD} > 0$ , see (Fig. 4b). The single current step at  $V_{SD} > 0$  in the  $D^-$  conducting region indicates a particular deviation from the sequential tunneling transport, as we will show later on.

Our experimental results regarding the orbital spectrum are thus as follows. We have measured a first excited state ( $n = 2$ ) at  $\sim 1$  meV by the temperature dependence. We cannot distinguish this state in the stability diagram due to insufficient resolution. An inspection of the current traces (see Fig. 4c) does show a very broad step starting at 7.5 meV and reaching its maximum height at around 15 meV. This broad step points at an ensemble of states entering the bias window that cannot be distinguished separately. This is confirmed by the trace at  $V_{SD} > 0$  where the single step is much narrower than at the other polarity and must belong to one of the states of this larger ensemble. There thus is (at least) one quantum state at around 7.5 meV ( $n = 3$ ) an another one at about 10 meV ( $n = 4$ ).

Next, we have performed tight-binding calculations in NEMO-3D of the  $D^-$  orbital spectrum, see Appendix II. Initial investigations of the effect of field confinement on the  $D^-$  state were carried out in Refs [43, 44], and more recently the effect of the interface on charging energy of the  $D^-$  state was investigated [35]. The only input parameters in our tight-binding method are the donors distance from the  $\text{SiO}_2$  interface ( $d$ ) and the local electric field ( $F$ ). These parameters were extracted from the donors  $D^0$ -spectrum [3]. The calculations show a low first excited state at around 1 meV and a higher manifold of states, which starts at around 7 meV. However, the exact spectrum of this higher manifold of states depends strongly on donor depth  $d$ . These calculations thus reasonably agree with our experiments.

The  $n = 4$  -state is the only one in the *entire* spectrum (both  $D^0$  and  $D^-$ ) that shows a current step at  $V_{SD} > 0$ ,

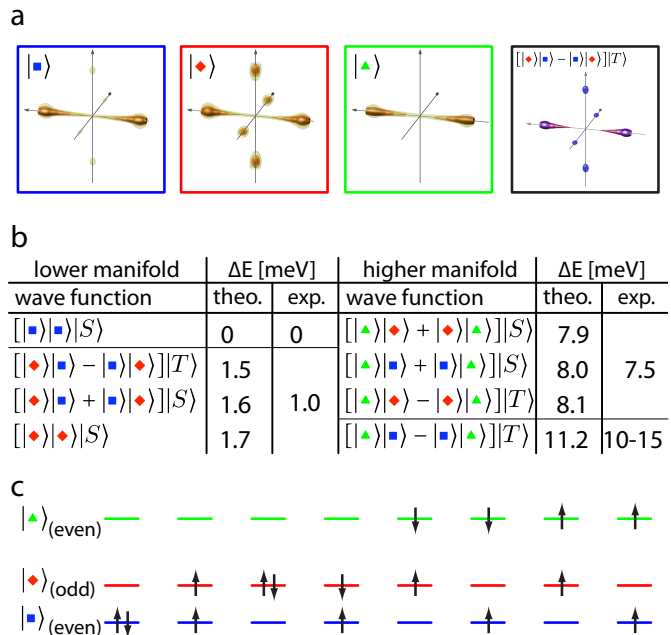


FIG. 5. Calculated spin valley configuration of the  $D^-$  level spectrum. (a) Single particle basis set from which the  $D^-$  spectrum is calculated, consisting of the ground state ( $|\square\rangle$ ), first excited state ( $|\diamond\rangle$ ) and second excited state ( $|\triangle\rangle$ ), derived from the  $D^0$  spectrum. Both the valley index (even or odd) and the spin (up or down) of each level of the single particle basis is indicated. (b) Result of the Hartree-Fock Tight-binding calculations. Each two electron state consist of a combination of two single particle-levels. (c) The spin-valley configuration.

a peculiar feature we can relate to its spin/valley nature, as we will show next.

With our degree of asymmetry, the maximum magnitude of any current step ( $n > 1$ ) in  $V_{SD} > 0$  equals 0.5% of the step at  $n = 1$ , regardless of  $\Gamma^n$ . The latter follows directly from Eq. 1 in combination with the asymmetry  $\Gamma_L/\Gamma_R \approx 2000$  we found from the temperature dependent data. That leads us to the conclusion that the sequential limit does not hold for  $n = 4$ , which thus means that an electron entering this state does *not* relax back to the ground state before exiting the atom. Since the  $n = 4$  -state does not relax back to the ground state, the life-time ( $\tau$ ) should be larger than the exiting rate, i.e.  $\tau > \Gamma_R^3$  (see Fig. 4d). By the magnitude of the current steps at  $V_{SD} < 0$  we can (conservatively) estimate  $\Gamma_R^3 \sim \Gamma_R^1$ , thus  $\tau > 48$  ns. Similar transport phenomenon have been observed in silicon double quantum dots due to spin-blockade (dubbed life-time enhanced transport) [18]. Similar influences of in-elastic transport were also predicted for silicon quantum dots under high applied bias [40].

To investigate the spin/valley nature of the donors  $D^-$  state, we calculate the spectrum in a self-consistent field

Hartree Fock method with tight-binding in Fig. 5. We start with a spin-degenerate single-particle basis, which is derived from the sample's  $D^0$  spectrum [3]. Due to the 2D symmetry imposed by the high gate field, the lowest two orbital states ( $|\square\rangle$  and  $|\diamond\rangle$ ) are linear combinations of the perpendicular valleys (along  $k_z$ ) split by the valley-orbit interaction as depicted in Fig. 5a. We will refer to the ground state as the “even” combination of valleys and the first excited state as the “odd” combination of valleys, although the exact  $k_z$ -valley composition is unknown. It should be noted that by plotting the relevant wavefunctions, we observe that state  $|\Delta\rangle$  is a QD-type state (see Fig. 2) bound by the barriers in the access region. State  $|\Delta\rangle$  is strongly 2D confined and (as the lowest QD-state) is of even valley configuration. We then consider all possible electronic configurations of this 6-state system, as given by 15 two-electron Slater determinants [46]. Since it is computationally intractable to perform a full configuration interaction with many 1e TB wavefunctions (basis functions) each representing about a million atoms, we adopt a scheme in which the 1e basis functions are updated iteratively with a Hartree-Fock mean-field potential obtained from each electronic configuration. In other words, each of the 15 two-electron configurations is iterated separately for self-consistency between charge and potential until convergence is reached. We chose this approach in this atomistic 2e system because the overall potential can be sensitive to the particular 1e levels the electrons occupy, and a general Kohn-Sham solution is likely to give a poor description of the excited 2e configurations. The results are plotted in Fig. 5b and Fig. 5c for the first 14 spin/valley combinations (8 excluding degeneracy). The occupation energy  $E_{ij}$  corresponds to the energy needed to add the second electron to state  $j$  with the first electron in state  $i$ . Figure 5-b and -c do not list all the states in the higher manifold ( $> 7$  meV), but that is not relevant here.

We find that the exchange energy between singlet and triplets are significant between electrons in the same valleys (i.e. compare  $|\Delta\rangle|\square\rangle + |\square\rangle|\Delta\rangle$ S with  $|\Delta\rangle|\square\rangle + |\square\rangle|\Delta\rangle$ T), but small for electrons in different valleys (i.e. compare  $|\Delta\rangle|\diamond\rangle + |\diamond\rangle|\Delta\rangle$ S with  $|\Delta\rangle|\diamond\rangle + |\diamond\rangle|\Delta\rangle$ T). Hada and Eto [47] have already predicted that in a system with such a spacial symmetry, the exchange interaction between electrons in different (combinations of)  $k_z$ -valleys would disappear. We can find more experimental evidence for the vanishing of exchange interaction between different valley states in our system from the magnetic field dependence of the valley Kondo effect of similar samples, see Ref. [48].

The lower manifold of states ( $< 2$  meV) does not contain a state with a triplet spin- and same (even-even or odd-odd) valley -combination, as triplet spin is not possible within one and the same valley. The first triplet spin- same valley -configuration state in the spectrum is

theoretically at 11.2 meV ( $|\Delta\rangle|\square\rangle + |\square\rangle|\Delta\rangle$ T, see Fig. 5b). This particular state can not relax back to any of the lower states in the spectrum, before either flipping spin (triplet to singlet) or flipping valley configuration (even-even to odd-even). The  $|\Delta\rangle|\square\rangle + |\square\rangle|\Delta\rangle$ T states are very close in energy to the experimental  $n = 4$ -lifetime enhanced state at 10 meV.

The singlet-triplet relaxation in bulk  $D^-$  donors is quite slow ( $\sim$  ms) however, the vicinity of the Si/SiO<sub>2</sub> interface is expected to reduce that time-scale. We can put a (conservative) lower bound on the singlet-triplet relaxation in our system by comparing it to the T1-time of 400 nm dots defined in a two-dimensional Si/SiO<sub>2</sub> electron system measured by spin echo [49], which was about 460 ns. Furthermore, the relaxation time from a state with one valley combination to the other can also be longer than 48 ns. In a silicon 2D confined geometry, valley-lifetimes in the order of  $\mu$ s are to be expected [25].

Based on this evidence, we thus conclude that the lifetime-enhanced transport we observe is due to a state with triplet spin- and same valley -configuration, present in the higher manifold of states.

From these initial measurements of the spectrum of a two-electron atom in a silicon host we have uncovered new aspects of atomic systems with restricted momentum space. As we have shown, the valley index forms a two level system in 2D-confined geometries that can serve as a pseudo-spin. Apart from the atomic physics that apply to this single donor system, the symmetry of the silicon host lattice thus adds another selection rule. Just as it where a regular spin, this valley degree of freedom could potentially serve as a qubit in quantum computation schemes. Such a scheme is unfortunately not technologically viable yet, as it would require precise control over the valley configuration of levels and a means of rotating the qubit coherently [25]. However, the valley index has the strong advantage that coherent quantum operations can be performed by electrically addressing the system instead of using AC-magnetic fields.

We acknowledge financial support from the EC FP7 FET-proactive NanoICT projects MOLOC (215750) and AFSiD (214989), the Dutch Fundamenteel Onderzoek der Materie FOM, the Australian Research Council, the Australian Government, the U.S. National Security Agency (NSA) and the Army Research Office (ARO) under Contract No. W911NF-04-1-0290. The work at Purdue and JPL is supported by grants from the Army Research Office. The work described in this publication was carried out in part at the Jet Propulsion Laboratory, California Institute of Technology under a contract with the National Aeronautics and Space Administration. Sandia is a multiprogram laboratory operated by Sandia Corporation, a Lockheed Martin Company, for the United States Department of Energys National Nuclear Security Administration under Contract No. DE-AC04-94AL85000. The use of computational resources

provided by nanoHUB.org operated by the Network for Computational Nanotechnology, funded by the National Science Foundation are acknowledged.

## Appendix

### I. Temperature dependence of $D^-$

Here, we turn our attention to the temperature dependence and characterize the electronic transport, before analyzing the stability diagram (and thus the orbital states) of our two-electron system. We apply an analysis first described by Foxman *et al.* [38]. Figure 6a shows the zero bias  $D^0$ -resonance as a function of temperature. The resonances broaden with increasing temperature due to the temperature-dependent Fermi-Dirac distribution in the leads. The temperature dependent resonances all were fitted with a Gaussian peak shape too extract the Full-Width-Half-Maximum (FWHM) and the peak height ( $G_{MAX}$ ), see Fig. 6b and Fig 6c respectively. Both figures show a transition in the transport regime roughly around 5 K. Below this transition temperature,  $G_{MAX}$  decreases- and the the FWHM increases -linear with  $T$ . This specific temperature dependence fully characterizes the transport as being *sequential* and dominated by a single level (i.e. the ground state). The slope of the FWHM as a function of  $T$  is equal to  $3.2 \pm 0.2 k_b$ , very comparable to the theoretical value of  $3.5 k_b$ . The small discrepancy is attributed to a finite lifetime broadening in our system. Above the transition temperature, the slope of the FWHM as a function of  $T$  is equal to  $4.16 \pm 0.02 k_b$ , comparable to the theoretical value of  $4.35 k_b$  for transport dominated by multiple levels. The small discrepancy is attributed to the fact that the theoretical value holds for *equidistant* level spacing, which is (as we will see) certainly not the case in our system. The latter is furthermore reflected in the behavior of  $G_{MAX}$  as a function of  $T$ , which should be independent of  $T$  for equidistant level spacing but instead does have a certain slope (being different from the single level case). However, we *can* conclude that the transition temperature corresponds to the first excited state starting to contribute to the transport, which yields a splitting between the ground and first excited state of  $k_b T_C \sim 1$  meV.

We can furthermore derive the coupling of the ground state to the source and drain leads ( $\Gamma_L$  and  $\Gamma_R$  respectively) from the temperature dependence of ( $G_{MAX}$  below  $T_C$ , which is given by [39]

$$G_{MAX} = \frac{e^2}{4k_b T} \frac{\Gamma_L \Gamma_R}{\Gamma_L + \Gamma_R} \quad (5)$$

By fitting  $G_{MAX}$  below  $T_C$  to eq.5 we find  $\frac{\Gamma_L \Gamma_R}{\Gamma_L + \Gamma_R} = 4.2 \cdot 10^{13}$ . Next, we have estimated  $\Gamma (= \Gamma_L + \Gamma_R)$  from transport measurements at 300 mK, where  $\Gamma > k_b T$  and the transport is thus in the *coherent* regime. Here the FWHM of the  $D^0$  resonance is mainly lifetime-broadened, i.e.  $FWHM = \Gamma$  [50], and we found  $\Gamma = 173 \mu eV$ . Com-

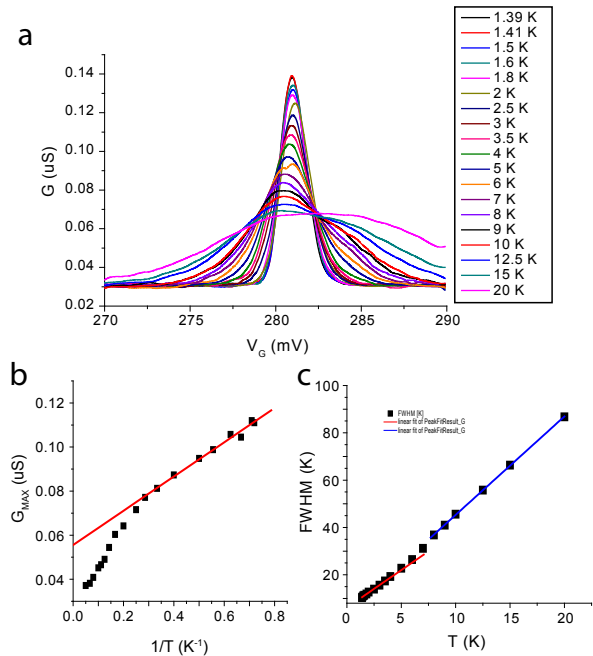


FIG. 6. Temperature dependence of the  $D^0$  resonance. **a)** Peak shape as a function of temperature. **b)** Peak height ( $G_{MAX}$ ) of the resonance as determined by a Gaussian fit to **a**. There is a change in the behavior  $\sim 5$  K, indicating the cross-over between the single-level- and the multi-level -regime **c)** Full-Width-Half-Maximum (FWHM) of the resonance as determined by a Gaussian fit to **a**. Again, there is a change in the behavior  $\sim 5$  K, indicating the cross-over between the two regimes.

binning the latter two pieces of information yields  $\Gamma_L = 173 \mu eV$  and  $\Gamma_R = 86 neV$ .

### II. $D^-$ level spectrum

Figure 7 shows the level spectrum of the  $D^-$  state of a single As donor positioned 4.9 nm and 5.4 nm from a  $SiO_2$  interface, calculated in a tight-binding approximation. For the local electric field and donor depth we expect in the experiment, we find a lower excited state at around 1 meV and a higher manifold starting at around 7 meV. We divide the level spectrum into a lower manifold (ground state and first excited state) and a higher manifold (second- to fifth -excited state). The states of the higher manifold depend strongly on local electric field and donor depth.

The transport experiment yields the difference between the ground state and any higher excited state, as it gives a contribution to the transport (step in the source-drain current) at the aforementioned energy spacing [3, 51]. Although transitions between excited states in principle also show up in Coulomb blocked transport, there contribution is typically much smaller [52].

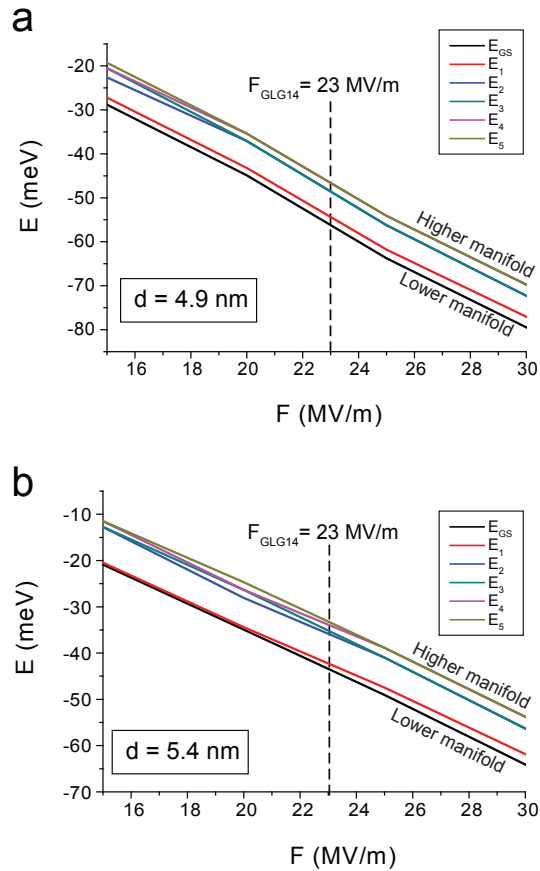


FIG. 7. Calculated level spectrum of the  $D^-$  resonance of a gated donor as a function of electric field ( $F$ ) by means of a tight-binding approximation. For clarity, only the lowest 6 states are shown. The exact spectrum for  $E_2$  and higher states is very dependent on the donor depth  $d$ , as can be observed from the differences between a)  $d=4.9$  nm and b)  $d=5.4$  nm. From previous research we estimate  $d=5.2$  nm and  $F=23$  MV/m in this sample (GLG14).

\* glansbergen@yahoo.com

[1] Sellier, H. *et al.*, Transport Spectroscopy of a Single Dopant in a Gated Silicon Nanowire, *Phys. Rev. Lett.* **97**, 206805 (2006)

[2] Calvet, L.E., Snyder, J.P., and Wernsdorfer, W., Excited-state spectroscopy of single Pt atoms in Si, *Phys. Rev. B* **78**, 195309 (2008)

[3] Lansbergen, G.P. *et al.*, Gate induced quantum confinement transition of a single dopant atom in a Si FinFET, *Nature Physics* **4**, 656 (2008)

[4] Tabe, M., *et al.*, Observation of discrete dopant potential and its application to Si single-electron devices, *Thin Solid Films* **518** S38S43 (2009)

[5] Pierre, M., Wacquez, R., Jehl, X., Sanquer, M., Vinet, M. and Cueto, O., Single-donor ionization energies in a

nanoscale CMOS channel, *Nature Nanotech.* **5**, 133-137 (2010)

[6] Tan, K.Y. *et al.*, Transport Spectroscopy of Single Phosphorus Donors in a Silicon Nanoscale Transistor, *Nano Lett.* **10**, 11-15 (2010)

[7] Tabe, M., *et al.*, Single-Electron Transport through Single Dopants in a Dopant-Rich Environment, to be published in *Phys. Rev. Lett.* (2010)

[8] Ruess, F. *et al.*, Realization of atomically controlled dopant devices in silicon. *Small* **3**, 563-567 (2007)

[9] S. R. Schofield *et al.*, Atomically Precise Placement of Single Dopants in Si, *Phys. Rev. Lett.* **91**, 136104 (2003)

[10] Jamieson, D. N. *et al.*, Controlled shallow single-ion implantation in silicon using an active substrate for sub-20-keV ions, *Appl. Phys. Lett.* **86**, 202101 (2005)

[11] Khalafalla M.A.H., Ono Y., Nishiguchi K. and Fujiwara, A., Identification of single and coupled acceptors in silicon nano-field-effect transistors, *Appl. Phys. Lett.* **91**, 263513 (2007)

[12] Gruber, A., Draebenstedt, A., Tietz, C., Fleury, L., Wrachtrup, J., von Borczyskowski, C., Scanning Confocal Optical Microscopy and Magnetic Resonance on Single Defect Centers, *Science* **276**, 2012 - 2014 (1997)

[13] Yakunin, A.M. *et al.*, Spatial structure of an individual Mn acceptor in GaAs, *Phys. Rev. Lett.* **92**, 216806 (2004).

[14] Kitchen, D., Richardella, A., Tang, J.-M., Flatte, M.E. and Yazdani, A., Atom-by-atom substitution of Mn in GaAs and visualization of their hole-mediated interactions. *Nature* **442**, 436439 (2006).

[15] Fuechsle, M., Mahapatra, S., Zwanenburg, F.A., Friesen, M., Eriksson, M.A, Simmons, M.Y., Spectroscopy of few-electron single-crystal silicon quantum dots, to be published in *Nature Nanotechnology*, doi:10.1038/nnano.2010.95

[16] Andresen, S.E.S. *et al.*, Charge State Control and Relaxation in an Atomically Doped Silicon Device, *Nano Lett.* **7**, 20002003 (2007)

[17] Thomas, G.A., Capizzi, M., DeRosa, F., Bhatt, R.N. and Rice, T.M., Optical study of interacting donors in semiconductors, *Phys. Rev. B* **23**, 54725494 (1981)

[18] Shaji, N. *et al.*, Spin blockade and lifetime-enhanced transport in a few-electron Si/SiGe double quantum dot, *Nature Physics* **4**, 540 (2008)

[19] Kane, B.E., A silicon-based nuclear spin quantum computer, *Nature* **393**, 133-137 (1998).

[20] Kane, B.E. *et al.*, Single-spin measurement using single-electron transistors to probe two-electron systems. *Phys. Rev. B* **61** (4) 2961-2972 (2000)

[21] Andresen, S.E.S. *et al.*, Charge state control and relaxation in an atomically doped silicon device. *Nano Lett*, **7**, 2000-2003 (2007)

[22] Vrijen, R., *et al.*, Electron-spin-resonance transistors for quantum computing in silicon-germanium heterostructures, *Phys. Rev. A* **62**, 012306 (2000)

[23] Hollenberg, L.C.L. *et al.*, Charge-based quantum computing using single donors in semiconductors, *Phys. Rev. B* **69** 113301 (2004)

[24] Hollenberg, L.C.L., Greentree, A.D., Fowler, A.G. and Wellard, C.J., Two-dimensional architectures for donor-based quantum computing, *Phys. Rev. B* **74**, 045311 (2006)

[25] Culcer, D., Cywiński, Li, Q., Hu, X., Das Sarma, S., Quantum dot spin qubits in Silicon: Multivalley physics, *arXiv:1001.5040v1 [cond-mat.mes-hall]*



- [26] Goswami, S. *et al.*, Controllable valley splitting in silicon quantum devices, *Nature Physics* **3**, 41-45 (2007)
- [27] Srinivasan, S., Klimeck, G. and Rokhinson L.P., Valley splitting in Si quantum dots embedded in SiGe, *Appl. Phys. Lett.*, **93**, 112102 (2008)
- [28] Neerav Kharche, N., Prada, M., Boykin, T.B., and Klimeck, G., Valley splitting in strained silicon quantum wells modeled with 2 degree miscuts, step disorder, and alloy disorder, *Appl. Phys. Lett.* **90**, 092109 (2007)
- [29] Timothy B. Boykin, T.B. *et al.*, Valley splitting in strained silicon quantum wells, *Appl. Phys. Lett.* **84**, 115-117 (2004)
- [30] Timothy B. Boykin, T.B. *et al.*, Valley splitting in low-density quantum-confined heterostructures studied using tight-binding models, *Phys. Rev Lett. B* **70**, 165325 (2004)
- [31] Takashina, K., Ono, Y., Fujiwara, A., Takahashi, Y., and Hirayama Y., Valley Polarization in Si(100) at Zero Magnetic Field, *Phys. Rev. Lett* **96**, 236801 (2006)
- [32] Boeuf, F., Jehl, X., Sanquer, M., and Skotnicki, T., Controlled single-electron effects in nonoverlapped ultrashort silicon field effect transistors, *IEEE Trans. Nanotechnol.* **2**, 144 (2003)
- [33] Jehl, X., Sanquer, M., Bertrand, G., Guegan, G., Deleonibus, S. and Fraboulet D., Silicon single electron transistors with SOI and MOSFET structures: The role of access resistances, *IEEE Trans. Nanotechnol.* **2**, 308 (2003)
- [34] Sellier, H. *et al.*, Subthreshold channels at the edges of nanoscale triple-gate silicon transistors, *Appl. Phys. Lett.* **90**, 073502 (2007)
- [35] Calderon, M.J., Verduijn, J., Lansbergen, G.P., Tetamanzi, G.C., Rogge, S., Koiller, B., Heterointerface effects on the charging energy of shallow  $D^-$  ground state in silicon: the role of dielectric mismatch, *arXiv:1005.1237v1 [cond-mat.mes-hall]*
- [36] Klimeck, G., Oyafuso, F., Boykin, T.B., Bowen, R.C. and von Allmen, P., Development of a Nanoelectronic 3-D (NEMO 3-D) Simulator for Multimillion Atom Simulations and Its Application to Alloyed Quantum Dots, *Computer Modeling in Engineering and Science* **3**, 601-642 (2002).
- [37] Klimeck, G. *et al.*, Atomistic Simulation of Realistically Sized Nanodevices Using NEMO 3-D: Part I - Models and Benchmarks, *IEEE Trans. Electron Dev.* **54**, 2079-2089 (2007)
- [38] Foxman, E.B. *et al.*, Crossover from single-level to multilevel transport in artificial atoms, *Phys. Rev. B* **50**, 1419314199 (1994)
- [39] Beenakker, C.W.J., Theory of Coulomb-blockade oscillations in the conductance of a quantum dot, *Phys. Rev. B* **44**, 1646-1656 (1991)
- [40] Klimeck, G., Lake, R., Datta, S. and Bryant, G., Elastic and Inelastic Scattering in Quantum Dots in the Coulomb Blockade Regime, *Phys. Rev. B* **50**, 5484 (1994)
- [41] Klein, M., Lansbergen, G.P., Mol, J.A., Rogge, S., Levine, R.D. and Remacle, F., Reconfigurable Logic Devices on a Single Dopant Atom: Operation up to a Full Adder by Using Electrical Spectroscopy, *ChemPhysChem* **10**, 162-173 (2009)
- [42] Castner, T.G., Raman Spin-Lattice Relaxation of Shallow Donors in Silicon, *Physical Review* **130**, 58-77 (1963)
- [43] Fang, A., Chang, Y.C., and Tucker, J., Effects of J-gate potential and uniform electric field on a coupled donor pair in Si for quantum computing, *Phys. Rev. B* **66**, 155331 (2002)
- [44] Hollenberg, L.C.L., Wellard, C.J., Fowler, A.G. and Pakes, C.I., Single-spin readout for buried dopant semiconductor qubits, *Phys. Rev. B* **69**, 233301 (2004)
- [45] Hatano, T., Stopa M. and Tarucha, S., Single-Electron Delocalization in Hybrid Vertical-Lateral Double Quantum Dots, *Science* **309**, 268-271 (2005)
- [46] Szabo A., and Ostlund, N.S. in *Modern Quantum Chemistry-Introduction to Advanced Electronic Structure Theory* (Dover Publications Inc.,1989).
- [47] Hada, Y., Eto, M., Electronic states in silicon quantum dots: Multivalley artificial atoms, *Phys. Rev. B* **68**, 155322 (2003)
- [48] Lansbergen, G.P. *et al.*, Tunable Kondo effect in a single donor atom, *Nano Lett.* **10**, 455460 (2010)
- [49] Tyryshkin, A.M. *et al.*, Electron spin coherence in Si, *Physica E* **35**, 257-263 (2006)
- [50] Büttiker, M., Coherent and sequential tunneling in series barriers, *IBM J. of Res. and Dev.* **32**, 6375 (1988).
- [51] Kouwenhoven, L.P. *et al.* in *Mesoscopic Electron Transport* (eds Sohn, L. L., Kouwenhoven, L. P. Schon, G.) (Kluwer, Dordrecht, 1997).
- [52] Pfannkuche, D. *et al.*, Selection Rules for Transport Excitation Spectroscopy of Few-Electron Quantum Dots, *Phys. Rev. Lett.* **74**, 1194-1197 (1995)